Nicotinic Acetylcholine Receptor Probed with a Photoactivatable Agonist: Improved Labeling Specificity by Addition of Ce^{IV}/Glutathione. Extension to Laser Flash Photolabeling†

Thomas Grutter, Maurice Goeldner, and Florence Kotzyba-Hibert*

Laboratoire de Chimie Bio-Organique, UMR 7514 CNRS, Faculté de Pharmacie−Université Louis Pasteur Strasbourg, 74 route du Rhin, BP 24, 67401 Illkirch Cedex, France

Received November 19, 1998; Revised Manuscript Received March 8, 1999

ABSTRACT: The molecular structure of *Torpedo marmorata* acetylcholine binding sites has been investigated previously by photoaffinity labeling. However, besides the nicotine molecule [Middleton et al. (1991) *Biochemistry 30*, 6987−6997], all other photosensitive probes used for this purpose interacted only with closed receptor states. In the perspective of mapping the functional activated state, we synthesized and developed a new photoactivatable agonist of nAChR capable of alkylation of the acetylcholine (ACh) binding sites, as reported previously [Kotzyba-Hibert et al. (1997) *Bioconjugate Chem. 8*, 472−480]. Here, we describe the setup of experimental conditions that were made in order to optimize the photolabeling reaction and in particular its specificity. We found that subsequent addition of the oxidant ceric ion (Ce^{IV}) and reduced glutathione before the photolabeling step lowered considerably nonspecific labeling (over 90% protection with *d*-tubocurarine) without affecting the binding properties of the ACh binding sites. As a consequence, irradiation at 360 nm for 20 min in these new conditions gave satisfactory coupling yields (7.5%). A general mechanism was proposed to explain the successive reactions occurring and their drastic effect on the specificity of the labeling reaction. Last, these incubation conditions can be extended to nanosecond pulsed laser photolysis leading to the same specific photoincorporation as for usual irradiations (8.5% coupling yield of ACh binding sites, 77% protection with carbamylcholine). Laser flash photocoupling of a diazocyclohexadienoyl probe on nAChR was achieved for the first time. Taken together, these data indicate that future investigation of the molecular dynamics of allosteric transitions occurring at the activated ACh binding sites should be possible.

The molecular structure of the *Torpedo marmorata* acetylcholine (ACh)[1] binding site has been probed by site-directed labeling and by site-directed mutagenesis. Topographical mapping of residues contributing to ACh binding on the *Torpedo* acetylcholine receptor (nAChR) was achieved with photosensitive irreversible probes which either were antagonists, [^{3}H]DDF (*1*, *2*) or [^{3}H]*d*-tubocurarine (*3*), or were agonists, [^{3}H]nicotine (*4*). From theses studies, three domains of the α-subunit centered around αTyr-93, αTrp-149 and αTyr-190, αCys-192, αCys-193, αTyr-198 have been identified. Residues γTrp-55 and δTrp-57 were also identified as the sites of specific [^{3}H]*d*-tubocurarine (*3*) and [^{3}H]nicotine (*5*) photoincorporation, demonstrating that other subunits (γ and/or δ) are associated to the α-subunit to form a functional agonist binding site.

The nAChR interconverts between at least four discrete conformational states upon agonist activation: resting, R; active, A; intermediate, I; and desensitized, D (*6*). Identification of the amino acids contributing to the architecture of the different nAChR conformational states will help to define, at the molecular level, the structural components necessary for agonist-induced changes in structure. As the transition from the resting (R) to the active state (A) takes place on a submillisecond time scale, photosensitive agonists, which generate rapidly and efficiently highly reactive species, are required in order to label irreversibly the ACh binding site in its transitory functional state (A). For this purpose, [^{3}H]-nicotine is not ideal because it suffers from extremely low labeling efficiency under equilibrium conditions (∼1%) (*4*). We recently developed a novel family of photosensitive agonists, of suitable size and reactivity, designed to incorporate instantaneously and covalently, upon irradiation, in surrounding residues (*7*). One of these photoprobes, DCTA (Figure 1), carrying, in addition to the quaternary ammonium group desirable for cholinergic recognition, a highly photosensitive 4-diazocyclohexa-2,5-dienone moiety was shown to be a functional agonist. [^{3}H]DCTA was synthesized and used to photoalkylate the ACh binding sites of *Torpedo* nAChR (*8*).

† This work was supported by the Centre National de la Recherche Scientifique, the Région Alsace, and the Association Française contre les Myopathies, Naturalia et Biologica.

* To whom correspondence should be addressed. E-MAIL: kotzyba@bioorga.u-strasbg.fr.

[1] Abbreviations: nAChR, nicotinic acetylcholine receptor; ACh, acetylcholine; CCh, carbamylcholine; DDF, *p*-(*N*,*N*-dimethylamino)-benzenediazonium fluoroborate; DCTA, diazocyclohexadienoylpropyl-trimethylammonium; HQTA, hydroquinoylpropyl-trimethylammonium; QTA, quinoylpropyl-trimethylammonium; α-BgTx, α-bungarotoxin; GSH, reduced glutathione; GSSG, oxidized glutathione; Ce^{IV}, cerium nitrate ammonium ($Ce^{IV}(NH_4)_2(NO_3)_6$); PMSF, α-toluylsulfonyl fluoride; PCP, phencyclidine; PEI, poly(ethylenimine); NPM, *N*-phenylmaleimide; NCB, noncompetitive blocker; PB, sodium phosphate buffer; R_t, retention time.

10.1021/bi982748o CCC: $18.00
Published on Web 05/20/1999

The photolabeling of the ACh binding sites, in the functional and transitory state (A) of the nAChR, represents a new challenge in dynamic photoaffinity labeling. Identification of the labeled amino acid(s) involved in such conformational transitions first requires the optimization of the yield and specificity of the photocoupling reaction using the photosensitive agonist [^{3}H]DCTA under photochemical conditions suitable for future experiments using rapid mixing techniques.

In the present paper, we analyze in detail the biochemical properties of [^{3}H]DCTA in the absence or presence of light on *Torpedo* nAChR. We demonstrate the significant role played by the photochemical side-products [^{3}H]HQTA and [^{3}H]QTA in the poor specificity of the photocoupling reaction between nAChR and [^{3}H]DCTA. We overcame these major drawbacks by quenching rapidly both side-products using subsequent addition of the oxidant ceric ion (Ce^{IV}) and reduced glutathione (GSH), leading to a very efficient and specific photolabeling reaction. A mechanism is proposed to take these experimental data into account and to provide a basis for understanding the side-reactions that might occur during the photocoupling reaction. We also show the efficacy of the scavengers Ce^{IV}/GSH in nanosecond pulsed laser photolabeling of nAChR leading to the same specific incorporation as for usual irradiation conditions.

MATERIALS AND METHODS

Materials. [^{3}H]DCTA ([^{3}H]diazocyclohexadienoylpropyltrimethylammonium, 0.7 Ci/mmol) was synthesized and purified as described previously (*8*). [^{3}H]QTA was obtained and purified as a secondary product of [^{3}H]DCTA (*8*). [^{3}H]-Phencyclidine ([^{3}H]PCP) and [^{125}I]α-bungarotoxin ([^{125}I]α-BgTx) were purchased from New England Nuclear. Small live *Torpedo marmorata* fishes were obtained from the Biological Station of Roscoff (France); electric organs were dissected, liquid nitrogen frozed, and stored at −80 °C. Pepstatin, aprotinin, PMSF, proadifen, carbamylcholine (CCh), *d*-tubocurarine chloride, reduced glutathione (GSH), and oxidized glutathione (GSSG) were purchased from Sigma. Cerium nitrate ammonium ($Ce^{IV}(NH_4)_2(NO_3)_6$) was purchased from Janssen.

Membrane Preparation. nAChR-rich membrane fragments were purified from *T. marmorata* frozen electric organs as described elsewhere (*9*) except that the buffer contained 50 mM PB, pH 7.5. Further purification was achieved by alkali treatment of nAChR-rich membrane fragments (*10*). Pepstatin and PMSF were dissolved in DMSO.

Specific [^{125}I]α-bungarotoxin binding was determined by the DEAE filter disk procedure and typically ranged from 3 to 4 nmol of [^{125}I]α-bungarotoxin bound/mg of protein (*11*). Protein determination was achieved by a modified Lowry method (*12*).

Saturation Experiments. The equilibrium binding of [^{3}H]-DCTA (0.7 Ci/mmol) to AChR-rich membranes in 10 mM PB, pH 7.2, was measured in the dark at room temperature by rapid filtration on GF-C filters (Whatman) preincubated for 1 h with 0.3% PEI at 4 °C. Binding experiments were performed as follow: nAChR-rich membranes (50 μg, 200 nM α-BgTx binding sites) were preincubated with 15 μM proadifen for 50 min in 500 μL of PB and equilibrated with various [^{3}H]DCTA concentrations for 20 min at 25 °C in the presence (when indicated) or absence of 500 μM Ce^{IV}/100 μM GSH. The binding reaction was quenched by dilution with 2.5 mL of cold PB, and the mixture was rapidly filtered through GF-C filters. The filters were washed twice with 2.5 mL of cold PB and were counted. Nonspecific binding was determined in the presence of 100 μM CCh added 30 min before equilibration with [^{3}H]DCTA and was a linear function of free [^{3}H]DCTA concentration at least up to 50 μM.

Competition Experiments. Ligand dissociation constants at the agonist binding site were determined in the dark, from the decrease in the initial binding rate of either *N. nigricollis* [^{3}H]α-neurotoxin (*13*, *14*) or [^{125}I]α-BgTx (when indicated) to nAChR-rich membranes (2−4 nM α-BgTx binding sites), both in their native and in their desensitized forms (about 75% in the D state with 15 μM proadifen pretreatment). Following simultaneous addition of 1 nM [^{3}H]α-neurotoxin and 0.5 μM−1 mM ligand, 0.3 mL aliquots were rapidly filtered (Millipore HAWP) at different times and counted. For [^{125}I]α-BgTx binding, nAChR-rich membranes were preincubated with or without 15 μM proadifen for 50 min at room temperature in 10 mM PB, pH 7.2, 100 mM NaCl, 0.01% Triton X-100. Various amounts of ligand (10 nM−1 mM) were added simultaneously with 2 nM [^{125}I]α-BgTx, and the samples were filtered (Millipore HAWP) after 6 min incubation at room temperature and counted. Dissociation constants of ligands for the noncompetitive blocker (NCB) binding site were measured (*15*) in the dark, from competition experiments at equilibrium between 1 nM [^{3}H]PCP and 10 μM−4 mM ligand using nAChR-rich membranes (68 nM [^{125}I]α-BgTx binding sites). The suspensions were filtered through GF-B (Whatman) and counted.

Binding experiments with the hydroquinone−glutathione conjugates were performed as follows: a solution of hydroquinone−glutathione conjugates was obtained from 50 μM HQTA/QTA 1:1 solution treated with Ce^{IV}/GSH (500 μM Ce^{IV} and 100 μM GSH) for 20 min at room temperature. To nAChR (2 nM) preincubated with proadifen in PB, 0.01% Triton X-100 was added simultaneously a solution of 33 μM hydroquinone−glutathione conjugates and 30 nM [^{125}I]α-BgTx. The samples were filtered after 6 min as described above, and the filters were counted. Nonspecific binding was performed in the presence of 100 μM CCh.

Competition Experiments in the Presence of Ce^{IV} and GSH. [^{125}I]α-BgTx *(11)* binding and [^{3}H]PCP *(15)* binding were performed at equilibrium in the presence or absence of 500 μM Ce^{IV} and 100 μM GSH. For [^{125}I]α-BgTx binding, values were determined from the slope of [^{125}I]α-BgTx binding to solubilized nAChR-rich membranes at equilibrium in 10 mM PB, pH 7.4, 1% Triton X-100. For [^{3}H]PCP binding experiments, a control with 100 μM proadifen was done to define nonspecific binding for the NCB site.

Photochemical Decomposition of DCTA: HPLC Identification of HQTA and QTA. A 10 μM aliquot of DCTA was irradiated with (when indicated) or without 500 μM Ce^{IV} and 100 μM GSH at 360 nm for 20 min in 600 μL of 10 mM PB, pH 7.2. In some experiments, nAChR-rich membranes (60 μg, 210 pmol, 0.35 μM α-BgTx binding sites) were added just before irradiation. A 500 μL aliquot was analyzed on an analytical Zorbax C18 HPLC column

(4.6 × 250 mm) coupled to a photodiode array (Waters 990). The column was eluted at 1 mL/min with a linear gradient from 100% solvent A (0.1% trifluoroacetic acid in H_2O) to 90% solvent A/10% acetonitrile for 30 min followed by a linear gradient from 90% solvent A/10% acetonitrile to 100% acetonitrile for 10 min. All solvents used were reagents of HPLC grade.

Photochemical Labeling of nAChR with [^{3}H]DCTA. A monochromatic light beam from a 1000 W Xe−Hg lamp (Hanovia) was focused on a quartz cell (1 cm path length) to form a spot 10 mm high and 2 mm wide. Irradiation experiments were carried out at 10 °C under magnetic stirring. *Torpedo* alkaline-treated membranes (60 μg, 210 pmol of α-BgTx binding sites) were suspended (600 μL) in 10 mM PB, pH 7.2, mixed with 10 μM [^{3}H]DCTA after preincubation with 15 μM proadifen (50 min at room temperature), and irradiated at 360 nm (30 μV) for 20 min. Protection experiments were carried out with prior addition of *d*-tubocurarine at room temperature (100 μM, 30 min), CCh (100 μM, 30 min), hexamethonium (100 μM, 30 min), or α-BgTx (625 nM, 90 min). Cerium nitrate ammonium (500 μM) and reduced glutathione GSH (100 μM) were added just before irradiation when needed. For *N*-phenylmaleimide (NPM)-nAChR alkylation, NPM dissolved in DMSO was preincubated 90 min in 10 mM PB, pH 7.2 (1 mM, final DMSO 0.55% v/v), at room temperature with nAChR-rich membranes (2.3 μM, 480 pmol of α-BgTx binding sites). The excess was removed by extensive dialysis (12 h), and the NPM-nAChR-alkylated membranes (210 pmol of α-BgTx binding sites) were irradiated as described previously.

Photolabeled nAChRs were recovered after one-step centrifugation at 11000*g* for 30 min at 4 °C. The pellets were solubilized in the sample buffer and analyzed on 10% SDS−PAGE. Radioactivity incorporated into each polypeptide chain was quantified after gel slicing, digestion, and counting (*16*). For fluorography, the 10% SDS−polyacrylamide gel was soaked in an Amplify (Amersham) solution and dried under vacuum. The gel was held in close contact with a Hyperfilm MP (Amersham) for 160 h at −80 °C, and then developed according to usual procedures.

Labeling of nAChR with [^{3}H]QTA. Alkaline-treated membranes were preincubated with 15 μM proadifen (50 min, 25 °C), and 10 μM [^{3}H]QTA (1.8 Ci/mmol) was then added with or without 100 μM CCh as described previously. The samples were either irradiated at 360 nm or incubated in the dark (20 min, 10 °C). After centrifugation, the pellets were solubilized and submitted to 10% SDS−PAGE. The radioactivity incorporated into each polypeptide chain was quantified after gel slicing, digestion, and counting.

Laser Flash Photolabeling of nAChR with [^{3}H]DCTA. For laser flash photolabeling, an excimer laser was operated at 351 nm (Xe-F_2-Ne-He) with a pulse energy of ca. 150 mJ and a pulse width of about 20 ns (frequency = 1 Hz). The 10 μM DCTA solution was irradiated with one laser pulse, and the samples were analyzed by UV before and after photolysis. *Torpedo* alkaline-treated membranes (60 μg, 210 pmol of α-BgTx binding sites) were suspended (600 μL) in 10 mM PB, pH 7.2, mixed with 10 μM [^{3}H]DCTA after preincubation with 15 μM proadifen (50 min at room temperature), and irradiated with one laser pulse (20 ns). Protection experiments were carried out with prior addition of CCh (100 μM, 30 min) or *d*-tubocurarine (100 μM, 30 min) at room temperature. Ce ^{IV} (500 μM) and GSH (100 μM) were added just before irradiation. Photolabeled nAChRs were recovered after one-step centrifugation at 11000*g* for 30 min at 4 °C. The pellets were solubilized in the sample buffer and analyzed on 10% SDS−PAGE. The radioactivity incorporated into each polypeptide chain was quantified after gel slicing, digestion, and counting.

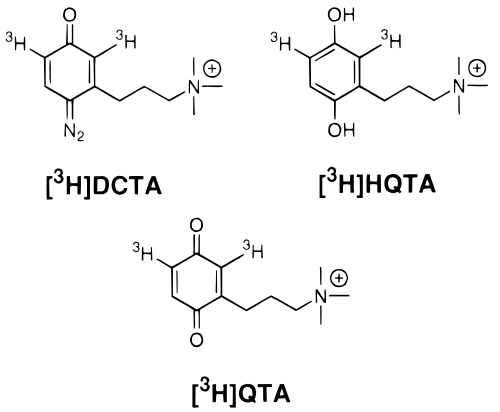

FIGURE 1: Structures of the photoactivatable probe [^{3}H]DCTA and the derived compounds [^{3}H]HQTA and [^{3}H]QTA.

Table 1: Physical and Binding Properties of Compounds DCTA, HQTA, and QTA

			ACh binding site K_p (μM)		NBC binding site K_i (μM)[c]
compound	λ_{max} (nm)	ϵ ($M^{-1}\cdot cm^{-1}$)	native form	with proadifen	with Carb
DCTA	349	26500	70 ± 10[a]	6.0 ± 0.9[a]	850 ± 150
HQTA	290	3000	4.5 ± 1.5[b]	9.5 ± 3.2[b]	nd[d]
QTA	250	8500	70 ± 8[a]	6.5 ± 0.5[a]	nd

[a] Protection constant (K_p) derived from [^{3}H]α-neurotoxin initial rate binding inhibition by tested ligands in the dark. [b] Protection constant (K_p) derived from [^{125}I]α-BgTx initial rate binding inhibition by tested ligands in the dark. [c] Inhibition constant (K_i) derived from [^{3}H]PCP binding inhibition by tested ligands at equilibrium in the dark. [d] Not determined.

RESULTS

Binding Properties of the Ligands DCTA, HQTA, and QTA. DCTA and its derivatives, HQTA and QTA (Figure 1), have micromolar affinities for the ACh binding site in the D state (after proadifen preincubation) with a 10-fold decrease in affinity for the native form, except for HQTA (Table 1). DCTA is highly selective for the ACh binding site compared to the NCB site, showing about 2 orders of magnitude difference in their respective affinities (D state). HQTA, the hydroquinone formed as the major product of DCTA photolysis during photolabeling experiments, showed an affinity for the ACh binding site similar to that of DCTA: K_p(HQTA) = 9.5 ± 3.2 μM versus K_p(DCTA) = 6.0 ± 0.9 μM. QTA, the quinone derivative formed from the oxidation of HQTA, also showed an affinity similar to DCTA and HQTA: K_p(QTA) = 6.5 ± 0.5 μM (Table 1).

[^{3}H]DCTA Equilibrium Binding. Equilibrium binding of [^{3}H]DCTA to nAChR-rich membranes was quantified to establish whether binding was specific for the agonist site and to determine equilibrium binding constants. Nonspecific binding in the presence of CCh (100 μM) and arecoline (100

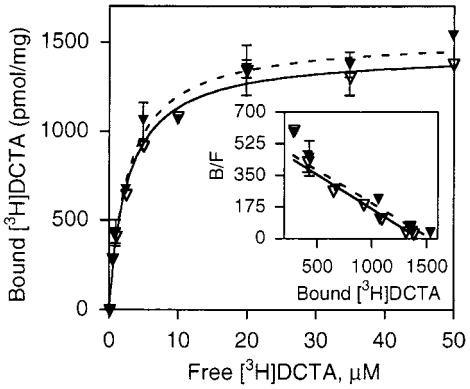

FIGURE 2: Binding of [^{3}H]DCTA to nAChR-rich membranes at equilibrium in the presence or absence of Ce^{IV}/GSH. nAChR-rich membranes (200 nM α-BgTx sites) were preincubated in the dark with 15 μM proadifen and equilibrated with various [^{3}H]DCTA concentrations for 20 min at 25 °C with or without 100 μM CCh (carbamylcholine) to define nonspecific binding, in the presence (▼ and dashed line) or absence (▽ and solid line) of 500 μM Ce^{IV}/100 μM GSH. The binding reaction was quenched by dilution with 2.5 mL of cold PB, and the mixture was rapidly filtered through GF-C filters pretreated with 0.3% PEI. Filters were washed twice with 2.5 mL of cold PB and counted. Inset: Scatchard plot. Symbols represent the average (±SD) of duplicate determinations, and the lines are fitted to the data by nonlinear and linear least-squares analysis for the saturation and Scatchard plots, respectively, according to a single-site model.

μM, not shown) increased linearly with free [^{3}H]DCTA concentration at least up to 50 μM. In the presence of proadifen (15 μM), the specific component of binding accounts for a single hyperbolic binding function, and the Scatchard representation allowed the determination of the following parameters: $K_D = 2.6 \pm 0.7$ μM, $B_{max} = 1412 \pm 89$ pmol/mg, $n_H = 1.0$ (Figure 2). The specifically bound [^{3}H]DCTA represents a single class of binding sites with no cooperativity as expected for desensitized ACh binding sites (after proadifen preincubation).

The dissociation constant of [^{3}H]DCTA for nAChR on the D state found for saturation experiments was in good agreement with values found in competition experiments with [^{125}I]α-bungarotoxin ($K_p = 6.0 \pm 0.9$ μM, Table 1). When [^{3}H]DCTA binding was measured in parallel with [^{125}I]α-BgTx binding, the number of [^{3}H]DCTA sites was similar to but less than the number of α-BgTx sites (72 ± 7%; $n = 4$). Furthermore, the stoichiometry of photocoupling was measured: 1.01 ± 0.04 mol of [^{3}H]DCTA was incorporated per mole of α-BgTx binding site inactivated (not shown). This indicates that [^{3}H]DCTA occupied both α-BgTx sites on nAChR, as expected for a nicotinic agonist.

Photolysis of DCTA: Identification by HPLC of Derived Ligands. The characterization and quantification of the photolysis products of DCTA were performed using C18 reverse-phase HPLC in the presence or absence of nAChR and under conditions used for the photocoupling between nAChR and [^{3}H]DCTA (with or without Ce^{IV}/GSH). No significant differences were observed in the presence or absence of nAChR (0.35 μM α-BgTx binding sites). After 20 min irradiation, more than 90% of DCTA was photolyzed either in the presence or in the absence of Ce^{IV}/GSH. Two products were identified in the absence of Ce^{IV} and GSH: the hydroquinone HQTA (47%, $R_t = 28$ min) and the quinone QTA (53%, $R_t = 34$ min) (Figure 3A). With 500 μM Ce^{IV}/100 μM GSH, no trace of HQTA or QTA was found but at least two peaks (peak 1, $R_t = 33$ min; and peak 2, $R_t = 42$ min) (Figure 3B) appeared corresponding to UV data of hydroquinone−glutathione conjugates *(17)*. In our experimental conditions (20 min irradiation), no trace of GSH oxidation (100 μM) into GSSG occurred as shown by comparative HPLC analysis (not shown).

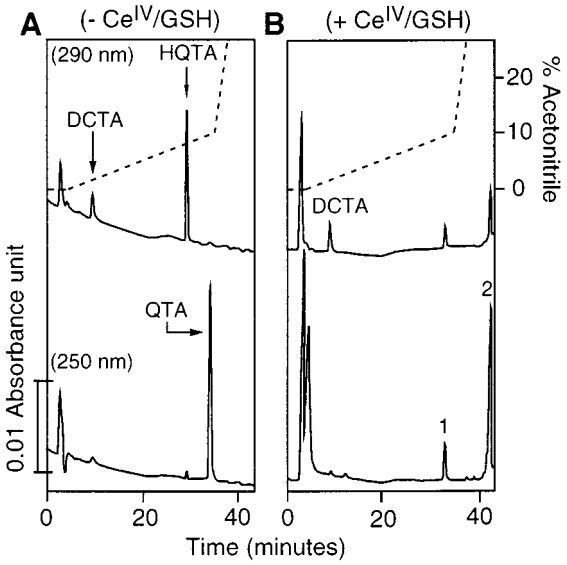

FIGURE 3: HPLC analysis of the products derived from DCTA photolysis. (A) 10 μM DCTA was irradiated at 360 nm for 20 min. An aliquot was analyzed on an analytical Zorbax C18 HPLC column coupled to a photodiode array. The column was eluted at 1 mL/min with a linear gradient from 100% solvent A (0.1% trifluoroacetic acid in H_2O) to 90% solvent A/10% acetonitrile for 30 min followed by a linear gradient from 90% solvent A/10% acetonitrile to 100% acetonitrile for 10 min. The chromatogram was visualized at 290 nm (upper trace) and 250 nm (lower trace). (B) The same experiment was done in the presence of 500 μM Ce^{IV}/100 μM GSH added before photolysis. (A) R_t (min): DCTA = 9, HQTA = 28, QTA = 34. (B) R_t (min): peak 1 = 33, peak 2 = 42.

Photolabeling of the ACh Binding Site Using [^{3}H]DCTA. Photolysis of [^{3}H]DCTA in the presence of *Torpedo* alkaline-treated nAChR, with or without protector, allowed us to quantify the radioactivity incorporated specifically into the different subunits. Without any protectors, the labeling pattern was broadly partitioned between all nAChR subunits (α, β, γ, and δ). Partial protection was observed on the α-subunits with different cholinergic agents such as CCh (30% protection). Nonspecific labeling occurred also on Na^+/K^+ ATPase, which was a minor impurity of the membrane preparation (Figure 4A). A series of controls were performed to understand and overcome this nonspecific labeling.

(i) nAChR/[^{3}H]QTA Labeling. [^{3}H]QTA, the quinone derivative of [^{3}H]HQTA, labeled covalently nAChR either in the presence (not shown) or in the absence of light (Figure 4A, inset). The labeling pattern was similar to that obtained for nAChR/[^{3}H]DCTA. No significant protection was observed with CCh.

(ii) NPM-nAChR/[^{3}H]DCTA Photolabeling. Pretreatment of *Torpedo* nAChR with NPM before photolabeling with [^{3}H]-DCTA greatly increased the specific labeling (from 30% to 67%, Figure 4B).

(iii) nAChR/[^{3}H]DCTA Photolabeling in the Presence of Ce^{IV} and GSH. Very minor labeling occurred (less than 10%) in the absence of light. Subsequent addition of the oxidant

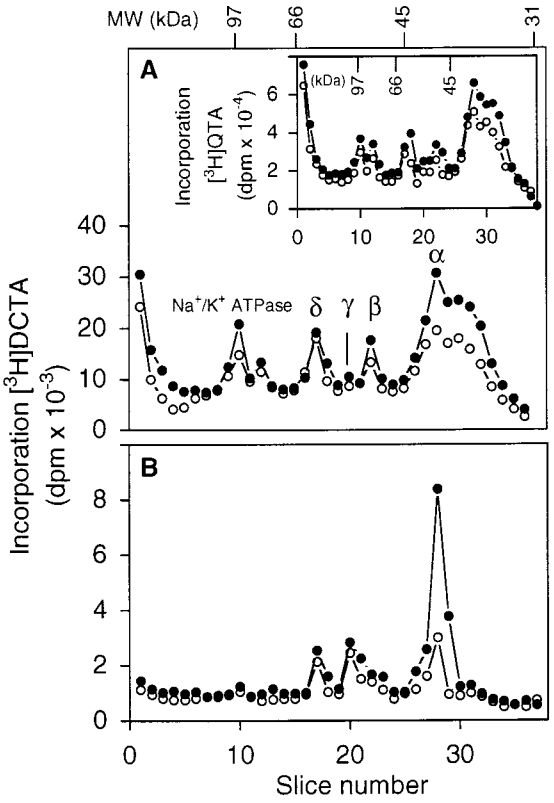

FIGURE 4: (A) SDS−PAGE analysis of [^{3}H]DCTA photoincorporation into alkaline-treated nAChR. Prior to irradiation, alkaline-treated membranes (210 pmol, 0.35 μM α-BgTx binding sites) were preincubated with proadifen for 50 min at room temperature. 10 μM [^{3}H]DCTA (0.7 Ci/mmol) was then added and irradiated at 360 nm for 20 min in the presence (○) or absence (●) of 100 μM CCh. After irradiation, the samples were centrifuged, and the pellets were subjected to 10% SDS−PAGE. Distribution of the radioactivity into the different subunits was measured after gel slicing, digestion, and counting. Inset: SDS−PAGE analysis of [^{3}H]QTA incorporation into alkaline-treated nAChR. Proadifen-preincubated alkaline-treated nAChRs (210 pmol, 0.35 μM α-BgTx binding sites) were incubated for 20 min in the dark with 10 μM [^{3}H]QTA (1.8 Ci/mmol) in the presence (○) or absence (●) of 100 μM CCh. (B) SDS−PAGE analysis of [^{3}H]DCTA photoincorporation into NMP-pretreated nAChR. Alkaline-treated membranes (480 pmol of α-BgTx binding sites) were preincubated for 90 min at room temperature with an excess of NPM (1 mM). The excess of NPM was removed by extensive dialysis. NPM-nAChR-alkylated membranes (210 pmol, 0.35 μM α-BgTx binding sites) were preincubated with proadifen for 50 min and irradiated with 10 μM [^{3}H]DCTA as mentioned above. Also indicated are the positions of the four nAChR subunits, the Na^+/K^+ ATPase minor impurity, and the molecular weight markers (MW in kDa).

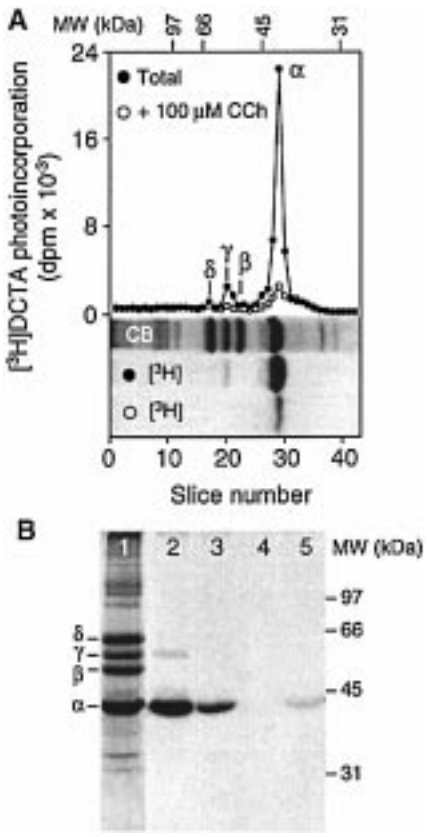

FIGURE 5: (A) Distribution of [^{3}H]DCTA photoincorporation into alkaline-treated nAChR in the presence of Ce^{IV}/GSH. Alkaline-treated membranes (210 pmol, 0.35 μM α-BgTx binding sites) were first preincubated with proadifen for 50 min at room temperature. 10 μM [^{3}H]DCTA, 500 μM Ce^{IV}, and 100 μM GSH were added successively and irradiated at 360 nm for 20 min in the presence (○) or absence (●) of 100 μM CCh. After irradiation, the samples were centrifuged (11000*g*, 30 min, 4 °C), pelleted, and subjected to 10% SDS−PAGE. Distribution of the radioactivity into the different subunits was measured after gel slicing, digestion, and counting. Corresponding Coomassie blue (CB) and fluorograph [^{3}H]: [^{3}H]DCTA photoincorporation in nAChR with (○) or without (●) 100 μM CCh. (B) SDS−PAGE of 10 μM [^{3}H]DCTA-photoalkylated nAChR in the presence of protectors. Corresponding Coomassie blue (lane 1) and fluorographs in the absence of protector (lane 2) or in the presence of 100 μM hexamethonium (lane 3), 100 μM *d*-tubocurarine (lane 4), and 625 nM α-BgTx (lane 5). Also indicated are the positions of the four nAChR subunits and the molecular weight markers (MW in kDa).

ceric ion and GSH in PB before nAChR photolabeling with [^{3}H]DCTA considerably decreased the overall nonspecific labeling as indicated by the low radioactivity background on total labeling profile (compare Figure 4A and Figure 5). Specific photolabeling on ACh binding sites was greatly increased involving principally the α-subunits [80 ± 5% protection by CCh (n = 3), 90 ± 5% by *d*-tubocurarine (n = 2), 64% by hexamethonium, and 91% by α-bungarotoxin; see Figure 5] and to a minor extent the γ-subunit [66 ± 4% protection by CCh (n = 3), 77 ± 5% by *d*-tubocurarine (n = 2), 52% by hexamethonium, and 79% by α-bungarotoxin; percentages were determined after gel slicing, digestion, and counting]. The presence of 10 μM PCP did not affect significantly the radioactivity photoincorporation on the α- and γ-subunits (not shown). The specific labeling was partitioned as follows: 93% of the specific radioactivity was found on the α-subunits and 7% on the γ-subunit. The yield of photoincorporation into the α-subunits was 7.6% of the total amount of ACh binding sites [7.6%: i.e., 16 pmol alkylated (24 000 dpm) per 210 pmol of ACh binding sites loaded on SDS−PAGE per lane].

Addition of reduced glutathione (GSH) in PB before nAChR photolabeling with [^{3}H]DCTA also increased specific labeling (78% protection with CCh, not shown). This increase of specific labeling was not observed with oxidized glutathione (GSSG, not shown). Controls were performed to ensure that in our experimental conditions in the presence of Ce^{IV}, GSH was not oxidized into GSSG.

In the absence of light, the pharmacological integrity of ACh and NCB binding sites was preserved under the experimental conditions used for photolabeling, i.e., Ce^{IV}/GSH addition. No loss of binding sites (α-BgTx or PCP) was observed in competition experiments (Figure 6), and no

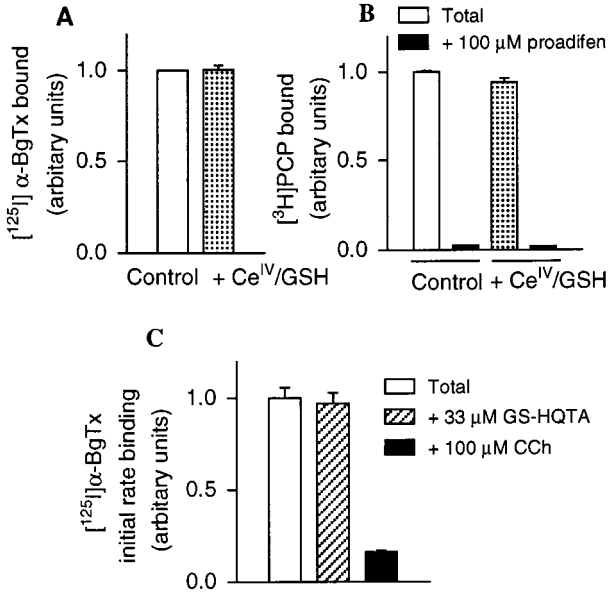

FIGURE 6: Binding controls on ACh and NCB binding sites in the presence of Ce^{IV}/GSH. (A) α-BgTx binding in the presence (stippled bar) or absence (white bar) of 500 μM Ce^{IV}/100 μM GSH. (B) [^{3}H]PCP binding in the presence (stippled bar) or absence (white bar) of 500 μM Ce^{IV}/100 μM GSH with (black bar) or without 100 μM proadifen to define nonspecific binding in PB. Data were normalized to the control and represent quadruplicate determinations (±SD). (C) Initial rate of binding of [^{125}I]α-BgTx in the presence (stippled bar) or absence (white bar) of 33 μM hydroquinone−glutathione conjugates (GS−HQTA). Nonspecific binding was measured with 100 μM CCh (black bar). Data were normalized to the control and represent triplicate determinations (±SD).

significant changes were detected in saturation experiments with [^{3}H]DCTA: $K_D = 2.7 \pm 0.5$ μM, $B_{max} = 1531 \pm 110$ pmol/mg, $n_H = 0.9$ (see dashed lines in Scatchard plot, Figure 2).

A binding control experiment with a hydroquinone−glutathione conjugate solution shows no significant reduction of the [^{125}I]α-BgTx binding sites in the presence of 33 μM of the conjugate solution: 95.6 ± 6.8 fmol of [^{125}I]α-BgTx binding sites was measured at 6 min in the presence of the scavenged species ($n = 3$) compared to 97.7 ± 6.2 fmol without. Nonspecific binding represents 16.0 ± 1.1 fmol of [^{125}I]α-BgTx binding sites with 100 μM CCh (Figure 6C).

Laser Flash Photolabeling of the ACh Binding Site with [^{3}H]DCTA. 10 μM DCTA was totaly photodecomposed after one laser pulse (20 ns, 351 nm, 150 mJ; see Figure 7A). Using the same irradiation conditions, nAChR/[^{3}H]DCTA was irradiated in the presence of Ce^{IV}/GSH which led to photoalkylation of the α- and γ-subunits protectable with CCh (77% protection on α-subunits and 70% protection on the γ-subunit, see Figure 7B) and with *d*-tubocurarine (85% protection on α-subunits and 62% protection on the γ-subunit, not shown). The extent of specific photolabeling (about 8.5%) was very similar to the one obtained at 360 nm in 20 min (7.5%, Figure 5). The specific labeling was partitioned as follows: 92% of the specific radioactivity was found on the α-subunits and 8% on the γ-subunit. No loss of ACh binding site was detected (less than 8%) after laser flash irradiation. When photolabeling was performed without Ce^{IV}/GSH, nonspecific labeling occurred on each subunit of nAChR and on Na^+/K^+ ATPase (not shown) as observed previously (Figure 4A).

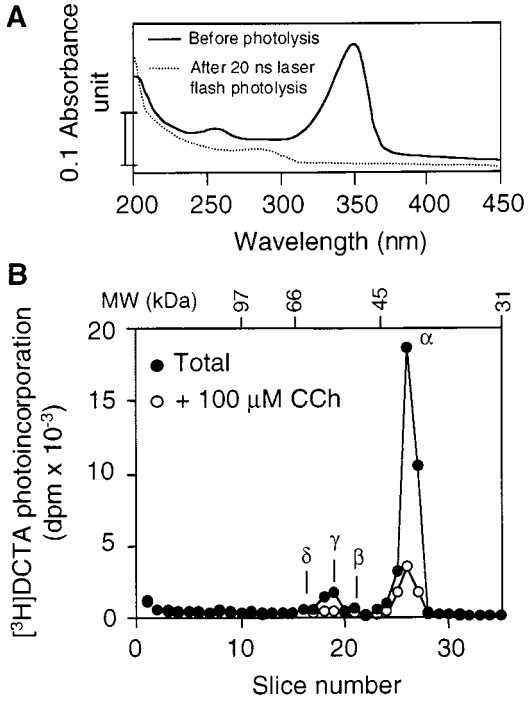

FIGURE 7: (A) Laser flash photolysis of DCTA. 10 μM DCTA was irradiated at 351 nm (150 mJ) with a 20 ns laser flash. The sample was analyzed by UV before (solid line) and after (dotted line) the 20 ns laser pulse. (B) Distribution of [^{3}H]DCTA photoincorporation into alkaline-treated nAChR in the presence of Ce^{IV}/GSH after 20 ns laser flash. Alkaline-treated membranes (210 pmol, 0.35 μM α-BgTx binding sites) were first preincubated with proadifen for 50 min at room temperature. 10 μM [^{3}H]DCTA, 500 μM Ce^{IV}, and 100 μM GSH were added successively and irradiated for 20 ns as described in (A) in the presence (○) or absence (●) of 100 μM CCh. After irradiation, the samples were centrifugated (11000*g*, 30 min, 4 °C), pelleted, and subjected to 10% SDS−PAGE. Distribution of the radioactivity into the different subunits was measured after gel slicing, digestion, and counting. Also indicated are the positions of the four nAChR subunits and the molecular weight markers (MW in kDa).

DISCUSSION

4-Diazocyclohexa-2,5-dienones are powerful probes able to efficiently photolabel enzymes (*18*) and receptor proteins (*7*, *19*) as well as to target specifically membrane-associated protein domains (*20*). We have used their photochemical properties to probe the agonist binding site of *Torpedo* nAChR. We showed earlier that DCTA (Figure 1) was a functional agonist able to irreversibly label the ACh binding site (*8*) under energy-transfer photochemical conditions (*21*). In this paper, we reinvestigated the photolabeling experiments in view of alkylating the active state A of the ACh binding site in suitable conditions, i.e., laser flash photolysis combined with rapid mixing techniques. With the energy transfer irradiation conditions (excitation of Trp residues around 290 nm) not being adapted for this purpose, we used the most energetic Xe−Hg irradiation wavelength at around 360 nm, close to the λ_{max} of DCTA (349 nm, Table 1), to ensure an efficient excitation process, and we worked out the reaction conditions to optimize the specificity of photolabeling.

Irradiation of the nAChR with the agonist [^{3}H]DCTA was performed at 360 nm in the presence of the NCB proadifen (15 μM) and at equilibrium, conditions where the receptor is mainly in the high-affinity D state [75% D, 25% R (*22*, *23*)]. This photocoupling gave rise to a broad labeling pattern

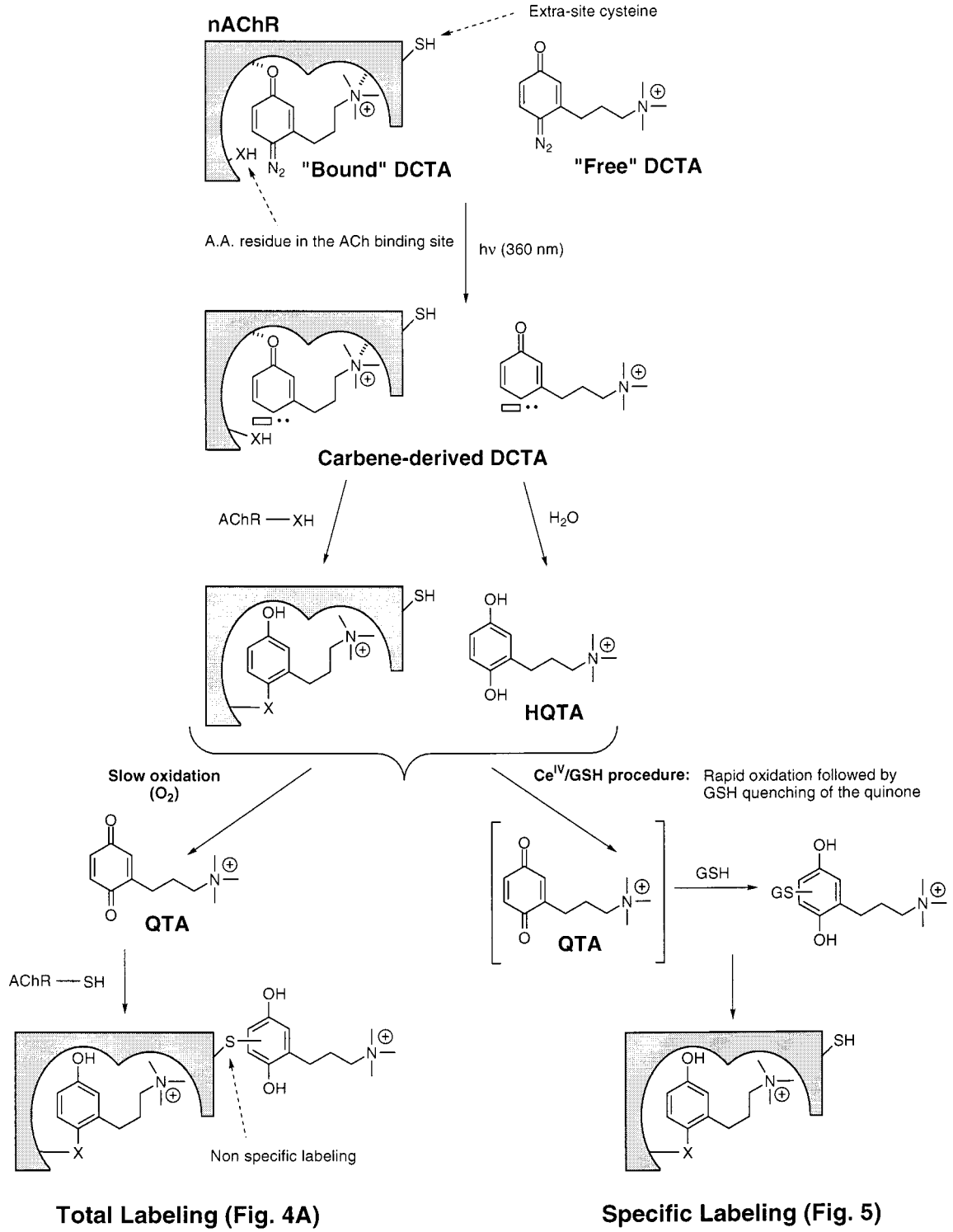

FIGURE 8: Hypothetical mechanism proposed for the photocoupling of the cyclohexadienoyl probe DCTA to nAChR. The carbonyl group and the charged quaternary ammonium mimic the pharmacophore, ensuring cholinergic recognition. X−H represents any amino acid belonging to the ACh binding site. Without Ce^{IV} and GSH addition, DCTA photoalkylation takes place in the ACh binding site (specific labeling) as well as QTA alkylation in extra-sites (nonspecific labeling) illustrated by a Cys nucleophilic residue. This gives the total labeling represented in Figure 4A. Subsequent addition of Ce^{IV} and GSH before photolabeling prevents nonspecific labeling: the hydroquinone HQTA photogenerated during the photocoupling between nAChR and DCTA was rapidly oxidized with Ce^{IV} into the quinone QTA which reacts with GSH to form hydroquinone−glutathione conjugates (Figure 5). Nonspecific alkylation of nAChR nucleophilic residues with QTA was prevented. The mechanism proposed here is the same for [^{3}H]DCTA photocoupling.

(Figure 4A) involving all the receptor subunits as well as the Na^+/K^+ ATPase, a minor impurity of *Torpedo* membrane preparations. The labeling of the α-subunits was only partially protectable with carbamylcholine (30% protection). A similar lack of labeling specificity could be observed on the $GABA_A$ receptor using diazocyclohexadienoyl ligands (*19, 24*).

The extent of nonspecific labeling observed suggested the involvement of secondary reactions occurring during the photolabeling experiment. Accordingly, we tested the pos-

sible role played by the photogenerated hydroquinone HQTA and quinone QTA derivatives in the limitation of the photolabeling process. As the photochemical reaction proceeds, these derivatives, which have similar affinities for the ACh binding site (micromolar range in the D state, see Table 1), progressively exert an in situ protection of the ACh binding sites from DCTA photoalkylation. Furthermore, quinones derived from catechols are known to covalently modify proteins; in particular, alkylation of the ACh binding site was described with the affinity redox reagent TMC (*25*).

To establish a possible role for the quinone QTA in the covalent coupling reaction with the nAChR, we incubated [^{3}H]QTA with nAChR. This experiment showed that radioactivity incorporation occurred in all receptor subunits, independently of the presence of light (not shown) and in a nonprotectable manner (Figure 4A inset). The radioactivity profile revealed by SDS−PAGE was similar to that of the photolabeling of the nAChR with [^{3}H]DCTA (Figure 4A).

To investigate the possible interference of cysteine residues in this nonspecific labeling, we pretreated the nAChR with the hydrophobic alkylating agent NPM in the absence of reducing agents. A large reduction of nonspecific labeling was observed (from 70% to 37%, Figure 4B), showing that [^{3}H]QTA acted as a nonspecific labeling agent generated during the photoreaction between nAChR and [^{3}H]DCTA. Na^+/K^+ ATPase labeling was also prevented by NPM treatment, providing evidence for sulfhydryl group interaction with [^{3}H]QTA and eventually with the ATP binding site of the catalytic subunit (*26*). The nonspecific labeling on nAChR possibly involved αCys-222 located on the transmembrane fragment M1 (and those in the homologous positions in the other subunits) accessible to NPM reagent (*27*, *28*). The other sulfhydryl groups located in the second intracellular loop of the γ-subunit are not accessible to NPM without detergent (*29*), and similarly [^{3}H]QTA is not able to label these residues according to the experimental procedure used here. As NPM is known to alter the functional properties of the nAChR channel (*30*), we could not use this pretreatment for the labeling of the active state A of the ACh binding site. An alternative solution was to rapidly quench [^{3}H]QTA formed during the photoaffinity labeling experiment, using the nucleophilic GSH (*17*). The results obtained were very similar to the NPM-pretreated nAChR allowing up to 78% protection with carbamylcholine (not shown).

A concomitant addition of Ce^{IV}/GSH to the reaction mixture induced a sequential oxidation/addition reaction of the side-products, the hydroquinone [^{3}H]HQTA and the quinone [^{3}H]QTA, respectively. This hydroquinone, derived from [^{3}H]DCTA photolysis, was rapidly oxidized with Ce^{IV} into the quinone [^{3}H]QTA which reacted subsequently with the nucleophilic thiol GSH to give hydroquinone−glutathione conjugates. Comparative HPLC analysis of the photolysis derivatives of DCTA in the absence or presence of Ce^{IV}/GSH confirmed this hypothesis (Figure 3). We checked (i) that this Ce^{IV}/GSH treatment did not affect either the binding of α-BgTx and PCP to the ACh and NCB binding sites, respectively (Figure 6), or [^{3}H]DCTA binding to nAChR in saturation experiments (Figure 2, dashed lines); and (ii) that hydroquinone−glutathione conjugates share no affinity for the ACh binding sites even at higher concentration (33 μM, Figure 6C). Figure 8 illustrates the reaction mechanisms taking place during the photolabeling experiments, according to the experimental data presented here.

This unusual experimental procedure offered several remarkable benefits for the photoaffinity labeling reaction. First, the reaction could be achieved on intact nAChR as shown in our control experiments. Second, the quenching of [^{3}H]HQTA and [^{3}H]QTA by Ce^{IV}/GSH allowed us to increase very strongly the specificity of the labeling reaction, allowing 80% overall protection with carbamylcholine and 90% and 91% protection with *d*-tubocurarine and α-bungarotoxin respectively (Figure 5). Finally, this procedure ensured an efficient removal of [^{3}H]HQTA and [^{3}H]QTA from the reaction mixture, preventing binding site occupancy, therefore leading to a higher photoincorporation. This procedure was extended to nanosecond pulsed laser photolysis of nAChR alkaline-treated membranes. One pulse of 20 ns induced photoalkylation of [^{3}H]DCTA into the ACh binding site (Figure 7B) comparable in efficacy and specificity to usual irradiation conditions (Figure 5).

In summary, we have characterized in some detail the capacity of the agonist DCTA to compete reversibly in the dark at the ACh binding site of the nAChR. We analyzed carefully the photochemical labeling reaction of the nAChR using [^{3}H]DCTA and showed in particular the side-product quinone [^{3}H]QTA as being directly responsible for the poor specificity of the labeling reaction. Treatment of the incubation mixture by Ce^{IV}/GSH led to an efficient and very specific labeling process, involving mainly the α-subunits with a smaller contribution of the γ-subunit of the nAChR. No labeling of the δ-subunit was detected with [^{3}H]DCTA as previously observed with [^{3}H]nicotine. Photocoupling using a laser irradiation source led to a satisfying similar specific incorporation of [^{3}H]DCTA into the ACh binding sites with the same efficiency as with a Xe−Hg lamp. This procedure allowed for the first time to photolabel specifically in 20 ns, with a laser source, the ACh binding sites with a diazocyclohexadienoyl agonist. These results are promising for future experiments using rapid mixing techniques.

The optimization in photocoupling between nAChR and the photosensitive agonist [^{3}H]DCTA applied to nanosecond pulsed laser experiments represents a decisive step toward resolution of the dynamic photolabeling of the nAChR. A more precise molecular understanding of conformational changes underlying the dynamic structural processes in cholinergic neurotransmission should be possible by comparing the topography of the ACh binding site before, during, and after agonist activation.

ACKNOWLEDGMENT

We thank Pr. J. Wirz and B. Hellrung for facilitating the laser experiments and Dr. K. Takeda for critically reading the manuscript.

REFERENCES

1. Dennis, M., Giraudat, J., Kotzyba-Hibert, F., Goeldner, M., Hirth, C., Chang, J. Y., Lazure, C., Chretien, M., and Changeux, J. P. (1988) *Biochemistry 27*, 2346−2357.
2. Galzi, J. L., Revah, F., Black, D., Goeldner, M., Hirth, C., and Changeux, J. P. (1990) *J. Biol. Chem. 265*, 10430−10437.
3. Chiara, D. C., and Cohen, J. B. (1997) *J. Biol. Chem. 272*, 32940−32950.
4. Middelton, R. E., and Cohen, J. B. (1991) *Biochemistry 30*, 6987−6997.

5. Chiara, D. C., Middleton, R. E., and Cohen, J. B. (1998) *FEBS Lett. 423*, 223−226.
6. Heidmann, T., Bernhardt, J., Neumann, E., and Changeux, J. P. (1983) *Biochemistry 22*, 5452−5459.
7. Kotzyba-Hibert, F., Kessler, P., Zerbib, V., Bogen, C., Snetkov, V., Takeda, K., Goeldner, M., and Hirth, C. (1996) *J. Neurochem. 67*, 2557−2565.
8. Kotzyba-Hibert, F., Kessler, P., Zerbib, V., Grutter, T., Bogen, C., Takeda, K., Hammadi, A., Knerr, L., and Goeldner, M. (1997) *Bioconjugate Chem. 8*, 472−480.
9. Saitoh, T., and Changeux, J. P. (1980) *Eur. J. Biochem. 105*, 51−62.
10. Neubig, R. R., and Cohen, J. B. (1979) *Biochemistry 18*, 5464−5475.
11. Schmidt, J., and Raftery, M. A. (1973) *Anal. Biochem. 52*, 349−354.
12. Peterson, G. L. (1977) *Anal. Biochem. 83*, 346−356.
13. Weber, M., and Changeux, J. P. (1974) *Mol. Pharmacol. 10*, 1−14.
14. Weber, M., and Changeux, J. P. (1974) *Mol. Pharmacol. 10*, 15−34.
15. Eldefrawi, A. T., Miller, E. R., Murphy, D. L., and Eldefrawi, M. E. (1982) *Mol. Pharmacol. 22*, 72−81.
16. Langenbuch-Cachat, J., Bon, C., Mulle, C., Goeldner, M., Hirth, C., and Changeux, J. P. (1988) *Biochemistry 27*, 2337−2345.
17. Lau, S. S., Hill, B. A., Highet, R. J., and Monks, T. J. (1988) *Mol. Pharmacol. 34*, 829−836.
18. Kessler, P., Ehret-Sabatier, L., Goeldner, M., and Hirth, C. (1990) *Tetrahedron Lett. 31*, 1275−1278.
19. Hawkinson, J. E., Goeldner, M. P., Palmer, C. J., and Casida, J. E. (1991) *J. Recept. Res. 11*, 391−405.
20. Alcaraz, M. L., Peng, L., Klotz, P., and Goeldner, M. (1996) *J. Org. Chem. 61*, 192−201.
21. Goeldner, M. P., and Hirth, C. G. (1980) *Proc. Natl. Acad. Sci. U.S.A. 77*, 6439−6442.
22. Krodel, E. K., Beckman, R. A., and Cohen, J. B. (1979) *Mol. Pharmacol. 15*, 294−312.
23. Heidmann, T., Oswald, R. E., and Changeux, J. P. (1983) *Biochemistry 22*, 3112−3127.
24. Kapfer, I., Hawkinson, J. E., Casida, J. E., and Goeldner, M. P. (1994) *J. Med. Chem. 37*, 133−140.
25. Gu, Y., Lee, H., Kirchhoff, J. R., Manzey, L., and Hudson, R. A. (1994) *Biochemistry 33*, 8486−8494.
26. Wallick, E. T., Lane, L. K., and Schwartz, A. (1979) *Annu. Rev. Physiol. 41*, 397−411.
27. Marquez, J., Iriarte, A., and Martinez-Carrion, M. (1989) *Biochemistry 28*, 7433−7439.
28. Kim, J., and McNamee, M. G. (1998) *Biochemistry 37*, 4680−4686.
29. Yee, A. S., Corley, D. E., and McNamee, M. G. (1986) *Biochemistry 25*, 2110−2119.
30. Clarke, J. H., and Martinez-Carrion, M. (1986) *J. Biol. Chem. 261*, 10063−10072.

BI982748O